Environmental Science & Technology

Article

pubs.acs.org/est

Ozonolysis of Trimethylamine Exchanged with Typical Ammonium Salts in the Particle Phase

Yanli Ge,[†,§] Yongchun Liu,[*,†,‡,§] Biwu Chu,[†,‡,§] Hong He,[†,‡,§] Tianzeng Chen,[†,§] Shaoxin Wang,[†] Wei Wei,[∥] and Shuiyuan Cheng[∥]

[†]State Key Joint Laboratory of Environment Simulation and Pollution Control, Research Center for Eco-Environmental Sciences, Chinese Academy of Sciences, Beijing, 100085, China

[‡]Center for Excellence in Urban Atmospheric Environment, Institute of Urban Environment, Chinese Academy of Sciences, Xiamen 361021, China

[§]University of Chinese Academy of Sciences, Beijing, 100049, China

[∥]Key Laboratory of Beijing on Regional Air Pollution Control, Beijing University of Technology, Beijing 100022, China

Supporting Information

ABSTRACT: Alkylamines contribute to both new particle formation and brown carbon. The toxicity of particle-phase amines is of great concern in the atmospheric chemistry community. Degradation of particulate amines may lead to secondary products in the particle phase, which are associated with changes in the adverse health impacts of aerosols. In this study, O_3 oxidation of particulate trimethylamine (TMA) formed via heterogeneous uptake of TMA by $(NH_4)_2SO_4$, NH_4HSO_4, NH_4NO_3 and NH_4Cl, was investigated with in situ attenuated total reflection Fourier transform infrared spectroscopy (ATR-FTIR) and proton transfer reaction mass spectrometry (PTR-MS). HCOOH, HCHO, $CH_3N{=}CH_2$, $(CH_3)_2NCHO$, CH_3NO_2, $CH_3N(OH)CHO$, CH_3NHOH and H_2O were identified as products on all the substrates based upon IR (one-dimensional IR and two-dimensional correlation infrared spectroscopy), quantum chemical calculation and PTR-MS results. A reaction mechanism was proposed to explain the observed products. This work demonstrates that oxidation might be a degradation pathway of particulate amines in the atmosphere. This will aid in understanding the fate of particulate amines formed by nucleation and heterogeneous uptake and their potential health impacts during atmospheric aging.

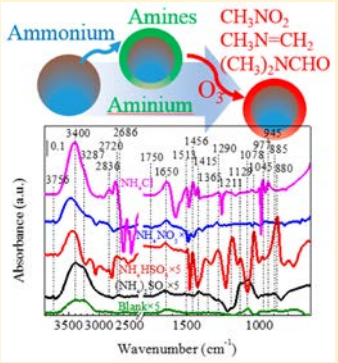

INTRODUCTION

Amines in the atmosphere are emitted from industrial processes, biomass burning, animal husbandry, automobile emissions, waste treatment facilities and marine emissions.[1] The atmospheric concentration of amines varies with location, and is typically 1−14 nmol Nm^{-3}, which is 1−2 orders of magnitude lower than that of ammonia.[1,2] In the atmosphere, amines can interconvert among gas-, liquid- and particle-phases through dissolution,[3] nucleation[4,5] and evaporation.[1] Novakov et al.[6] first reported the presence of amines in particulate matter in 1972, and subsequently more and more field measurements identified amines in atmospheric particles.[2,7−9] It has been suggested that amines may contribute up to 10−20% of the organic content of ambient particles, and frequently over one hundred different amine species containing 1−4 N atoms and ranging in MW from 59−302 Da have been observed in the particle phase.[2,10]

Amines play an important role in new particle formation (NPF) for the H_2SO_4−H_2O-amines ternary system and their subsequent growth,[11] in particular, in areas of where anthropogenic emission of amines are strong. For example, aliphatic amines contributed 23% to the NPF events at a remote forested site in Hyytiälä, Finland in March, 2006 and 47% to that at an urban site in Tecamac, Mexico in April, 2007.[12] Amines observed in Marshall Field Site, Colorado (2007),[13] North Boulder, Colorado (2009), and Atlanta, Georgia (2009)[14] have also been confirmed to play the same role in NPF events.[12] In laboratory studies, NPF was observed when amines were added into a smog chamber or flow tube reactor containing a certain concentration of nitric acid,[15] sulfuric acid,[16] or methanesulfonic acid (MSA).[17,18] Density functional theory (DFT) calculations indicated that amine molecules act as cluster stabilizers for nucleation precursors,[19,20] and therefore promote nuclei formation.[16,21] Heterogeneous uptake of amines by particles also contributes to particle-phase amines. Exchange or substitution reactions between amines and ammonium salts ($(NH_4)_2SO_4$, NH_4HSO_4, NH_4NO_3 and NH_4Cl) have been confirmed using both mass spectrometry[22] and Raman spectrometry.[23,24] The uptake coefficient (γ) of amines on coarse particles of ammonium salts is on the order of 10^{-3}−10^{-2},[23,25−27] while

Received: August 29, 2016
Revised: September 7, 2016
Accepted: September 14, 2016
Published: September 14, 2016

DOI: 10.1021/acs.est.6b04375
Environ. Sci. Technol. 2016, 50, 11076−11084

it is close to unity with nanoscale ultrafine particles.[22] The γ of amines on organic acids (citric acid and humic acid) via acid−base reaction is 10^{-5}−10^{-3} depending on the type of organic acid. It has been found that stronger acidity of particulate matter,[27] smaller steric effect with fewer substituted groups on the amines are favorable for the heterogeneous uptake of amines.[23] In addition, the uptake coefficient of amines on $(NH_4)_2SO_4$ particles is highly dependent on the metastable (efflorescence or deliquescence) state, which is determined by the relative humidity, of $(NH_4)_2SO_4$.[24] Heterogeneous uptake of amines on sulfate particles may considerably alter the aerosol properties, such as leading to a transition from the crystalline to an amorphous phase and increased water uptake, considerably enhancing their direct and indirect climate forcing effects.[28]

In the atmosphere, oxidation by OH was considered to be the main degradation pathway of amines. Their atmospheric lifetimes were estimated to be several hours based on the measured second-order rate constants ($(2-6) \times 10^{-11}$ cm^{-3}·$molecule^{-1}$·s^{-1}).[29] Oxidation by O_3 was another degradation path of amines. The lifetime for typical amines reacting with O_3 in the gas phase varies from several hours to around 10 days.[30] Oxidation of amines in the gas phase results in the formation of both volatile and condensed products.[31−33] For example, products including $(CH_3)_2NCHO$, $CH_3N{=}CH_2$, CH_3NO_2, HCHO, HCOOH, and CO_2 have been identified from ozonolysis of gas-phase trimethylamine (TMA).[34] It has also been found that significant nonsalt organics contributed to the secondary organic aerosol (SOA) from ozone oxidation and photooxidation of TMA and TEA.[15] Particulate amines and secondary oxidation products from amines in the particle phase are associated with adverse aerosol health impacts. For example, concentrations of 20 mL·m^{-3} trimethylamine were found to found to irritate the mucous membranes and eyes.[35] Alkylamines may also act as endogenous teratogens under certain conditions.[36,37] This implies that heterogeneous oxidation of particle-phase amines should subsequently modify their toxicity. A recent work has found that ozonolysis of particle-phase octadecylamine leads to nitroalkanes,[38] which are carcinogenic.[39] However, the further transformation or fate of particle-phase amines formed through heterogeneous uptake of short chain alkylamines is unclear. Therefore, it is important to study the degradation of particle-phase amines formed via nucleation and/or heterogeneous uptake under atmospheric conditions to understand their climatic and health impacts.

In this work, the heterogeneous ozonolysis of particulate TMA exchanged with typical ammonium salts found in atmospheric particles was investigated for the first time using an in situ attenuated total internal reflection infrared (ATR-IR) spectrometer as well as a proton transfer reaction mass spectrometer (PTR-MS). The degradation mechanism of particle-phase TMA by ozone was discussed. The results of this study will aid in understanding the fate of particulate amines formed by nucleation and heterogeneous uptake and their potential impacts during atmospheric aging.

EXPERIMENTAL SECTION

Chemicals. $(NH_4)_2SO_4$, NH_4HSO_4, NH_4NO_3 and NH_4Cl were used to simulate the typical ammonium components in atmospheric particles. $(NH_4)_2SO_4$ (≥99.0%), NH_4HSO_4 (41.5−43.5% H_2SO_4), NH_4NO_3 (≥99.0%), and NH_4Cl (≥99.5%) were used as received and supplied by Sinopharm Chemical Reagent Co. Ltd. TMA (28%) in aqueous solution was used as received from TCI. Ultrapure water (18.2 MΩ) was used to prepare ammonium salt solutions.

Heterogeneous Ozonolysis Experiments. Ozone oxidation of particle-phase TMA was performed in an in situ ATR reactor. The reaction chamber consisted of a ZnSe crystal and a sealed Teflon cover with entry and exit ports. The surface-to-volume ratio was 2 cm^{-1} with a volume of 44 cm^3. More details about the reactor was shown in the Supporting Information (Figure S1). The particles were prepared by depositing small droplets containing ammonium salts onto the ZnSe crystal with an atomizer, followed by purging with 1 L·min^{-1} zero air to obtain dry particles. The particle size for the generated ammonium salt particles was 115 ± 76 μm measured using a scanning electron microscope (SEM, Hitachi S3000N with an accelerating voltage of 10 kV). Although the particle size is 2−3 orders of magnitude greater than that of atmospheric particles, the reaction path obtained in this work should be credible because particle size has little influence on the reaction mechanism. Amorphous ammonium salt particles (several mg, Table S1) were obtained in this study.

After the particles were dried, which was monitored by observing the IR bands of water, TMA (~385 ppm) vapor was introduced into the reactor by a flow of 200 mL·min^{-1} zero air through a water bubbler containing TMA. The RH in the gas flow was 21% measured with a RH sensor (HMP110, HUMICAP). The IR spectra were collected with a time resolution of 1 min using the dried ammonium salts as reference. The exchange reaction was carried out until a dynamic equilibrium was established. Physically adsorbed and gaseous TMA as well as adsorbed water were removed by purging the sample with 1 L·min^{-1} zero air until the IR spectrum showed no further changes (around 2 h). Protonated TMA should be the initial form of TMA because the exchange reaction were performed under high TMA concentration for a long time and almost 100% exchange degree was observed in previous work under similar conditions.[24]

100−400 ppbv O_3 was introduced into the reactor to start the heterogeneous ozonolysis of particulate TMA. O_3 was generated by passing zero air through a quartz tube irradiated by a UV lamp (185 nm line dominated, Beijing Lighting Research Institute). The O_3 concentration in the gas flow was measured using an O_3 monitor (model 202, 2B Technologies). Because the mass of ammoniums deposited on the ZnSe crystal (Table S1) varied in each experiment, subsequently, leading to different amount of the particulate TMA exchanged. Therefore, it is reasonable to propose that the amount of exchanged TMA which was determined by the amount of deposited ammoniums on the ZnSe crystal, the equilibrium chemical compositions on different ammonium and the reactivity of particulate TMA toward O_3 should have influence on the concentrations of the surface species. The IR spectra with the best spectral quality were shown and qualitatively analyzed in this work to more confidently identify the surface products and to study the reaction mechanism. To further eliminate the possible influence of the trace TMA in gas phase or adsorbed on the walls of the reactor, the chamber was flushed with O_3 balanced in 100 mL·min^{-1} zero air for 15 min. Then, the inlet and outlet of the reactor were closed to for the oxidation reaction in a closed system. In situ IR spectra were recorded on a Nicolet 6700 (Thermo Nicolet Instrument Corporation) Fourier transform infrared (FT-IR) spectrometer equipped with an in situ attenuated total reflection chamber and a high sensitivity mercury cadmium telluride (MCT) detector cooled by liquid

DOI: 10.1021/acs.est.6b04375
Environ. Sci. Technol. 2016, 50, 11076−11084

N_2. The infrared spectra were collected and analyzed by a computer with OMNIC 6.0 software. All spectra reported here were recorded at a resolution of 4 cm^{-1} for 100 scans. A PTR-MS (500 HS, Ionicon Analytik)[40] was used to further identify the products by monitoring the composition of the outflow gas obtained by purging the oxidized sample with 1 $L{\cdot}min^{-1}$ of zero air after ozone oxidation was completed (12 h). Before that, mass spectra were also collected for comparison during purging of the TMA-exchanged ammonium salts with 1 $L{\cdot}min^{-1}$ of zero air before O_3 was introduced into the chamber. PTR-MS measures the molecular ions without substantial fragmentation or adduct formation and provides supplemental information about the products because it is a soft ionization technique.[41,42] Two-dimensional correlation spectroscopy (2DCOS) is an invaluable tool to elucidate the changes that occur at a molecular level when a system is subjected to external perturbation,[43,44] which obtains a higher spectral resolution by resolving the correlations into imaginary and real components and by distributing the peaks over a second dimension.[45,46] Therefore, it is capable of measuring small couplings and can be used as an incisive tool to shed light on the detailed structure and its structural change in time.[47] The 2DCOS was analyzed using SpectraCorr 2DCOS Software (Thermo Fisher Scientific).

Quantum Chemical Calculations. Quantum chemical calculations were performed using the Gaussian 09 program which is consistent with the IR assignments for the possible products during ozone oxidation. All geometry optimizations and vibrational frequency calculations were performed at the B3LYP hybrid DFT level of theory with the 6-311++G (d, p) basis set. A scaling factor of 0.975 was used to account for anharmonicity in the calculated vibrational frequencies based upon those products with known IR spectra (NIST).

RESULTS AND DISCUSSION

Exchange Reaction between TMA and Ammonium. An exchange reaction between TMA and $(NH_4)_2SO_4$ was conducted first to obtain particulate TMA. As shown in Figure 1, the typical IR bands of TMA, as confirmed with the NIST database, increased as a function of reaction time when the dried $(NH_4)_2SO_4$ was used as a reference. The peaks at 2960 and 2870 cm^{-1} are the asymmetrical stretching vibration of CH_3 ($\nu_{as}(CH_3)$) and the symmetrical stretching vibration of CH_3 ($\nu_s(CH_3)$), respectively, which are accompanied by the deformation vibration of CH_3 ($\delta(CH_3)$) at 1486 and 1446 cm^{-1} and the rocking vibration of CH_3 ($\rho(CH_3)$) from 985 to 1290 cm^{-1}.[48] The band at 845 cm^{-1} is assigned to overtone of asymmetrical deformation vibration of NC_3 ($2\delta_{as}(NC_3)$).[48] The peaks in the range of 2300−2700 cm^{-1} are the overtone/combination bands of − CH_3 and NC_3 groups, which have been well assigned in the literature.[48] During the exchange reaction, evidence of the adsorption of water, namely, ν_s(OH) (3400 cm^{-1}) and δ(OH) (1640 cm^{-1})[49] was also observed, because water vapor was present in the gases during bubbling. The absorption bands of water decreased markedly, whereas the peaks attributed to TMA (1289, 1230, 1160, 985, and 845 cm^{-1}) increased notably after the sample was purged for 2 h with zero air. This can be explained by the symmetry changes from solvated to dry aminium salts.

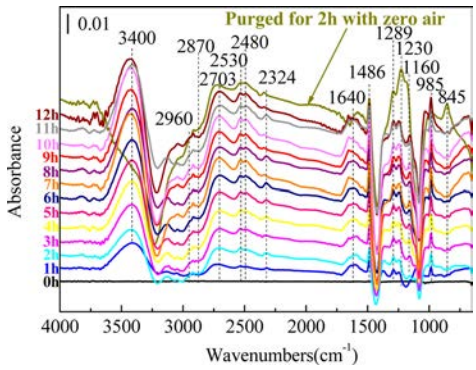

Figure 1. Time series of IR spectra during reaction between TMA and $(NH_4)_2SO_4$.

It should be noted that strong negative peaks at 3250 and 1420 cm^{-1} were also observed, as shown in Figure 1, when TMA was introduced into the reactor chamber. They are the typical $\nu_s(NH_4^+)$ (3250 cm^{-1}) and $\delta(NH_4^+)$ (1420 cm^{-1}) bands of $(NH_4)_2SO_4$,[50] respectively. This means that ammonium is replaced by TMA. The reaction is similar to a previous work where NH_3 has been identified as a gas-phase product of the reaction between methylamine and ammonium.[51] In Figure 1, the negative peak at 1080 cm^{-1} due to $\nu_s(SO_4^{2-})$[50] can be explained by a part of the sulfate transforming into bisulfate due to TMA or NH_3 evaporation from TMAH sulfate or $(NH_4)_2SO_4$ particles, which is similar to the transformation of TEAH sulfate to TEAH bisulfate observed using Raman spectroscopy.[24] On the other hand, a previous work found that the bands at 1484 and 984 cm^{-1} are the characteristic IR bands of protonated TMA ($(CH_3)_3NH^+$), both in solution and on the surface of polyethylene (PE).[52] These frequencies are almost the same as the observed IR bands at 1486 and 985 cm^{-1} in this study. This further confirmed that a substitution reaction took place between TMA and $(NH_4)_2SO_4$. As shown in Figure 1, the intensities for all of these IR bands increased slightly because the exchange rate between TMA and ammoniums gradually slowed down after 3 h of reaction. It should be noted that physisorbed TMA should be negligible compared with the chemically exchanged TMA ($TMAH^+$) because the intensity of the IR bands of the surface species, except for water and NH_4^+, did not decrease after the sample was purged with 1 $L{\cdot}min^{-1}$ of zero air for 2 h as shown in Figure 1.

The exchange reaction was also observed when NH_4NO_3 and NH_4Cl were individually exposed to TMA. The IR spectra are shown in Figure 2 after the ammonium salts reacted with TMA had been further purged with dry zero air for 2 h. The peaks attributed to $-CH_3$ (1486 cm^{-1}, $\delta(CH_3)$; 1289 cm^{-1}, 1230 and 985 cm^{-1}, $\rho(CH_3)$), NC_3 groups (816 cm^{-1}, $2\delta(NC_3)$) and the overtone/combination bands of − CH_3 and NC_3 groups in the range of 2300−2700 cm^{-1} were also observable.[48] At the same time, consumption of NH_4^+ was supported by the negative peaks of $\nu_s(NH_4^+)$ (~3200 cm^{-1}) and $\delta(NH_4^+)$ (1420 cm^{-1})[48] for both NH_4NO_3 and NH_4Cl (Figure 2) even though the strong negative peaks at ~3200 cm^{-1} make it difficult to discern the $\nu_{as}(CH_3)$ and $\nu_s(CH_3)$ bands on NH_4NO_3.

When NH_4HSO_4 was exposed to TMA, the negative peaks attributed to NH_4^+ were very weak, whereas the typical absorbance bands of TMA increased significantly. Additionally, a new peak centered at 1080 cm^{-1} due to $\nu_s(SO_4^{2-})$[50] increased, which means TMA had reacted with NH_4HSO_4 and existed on the crystal. This means an acid−base reaction instead of an exchange/displacement reaction should mainly take place between TMA and NH_4HSO_4. At the same time, this

DOI: 10.1021/acs.est.6b04375
Environ. Sci. Technol. 2016, 50, 11076−11084

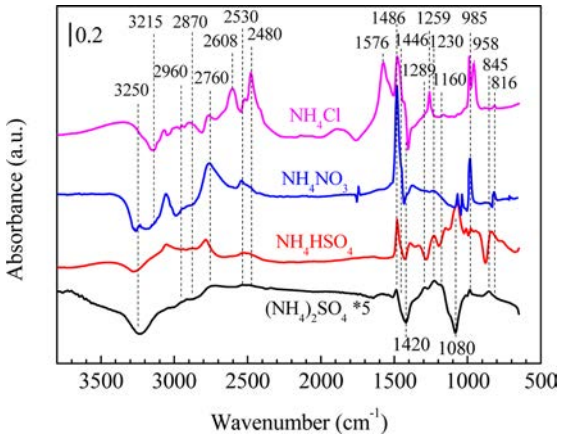

Figure 2. IR spectra after the reacted ammonium with TMA further purged with dry zero air for 2 h.

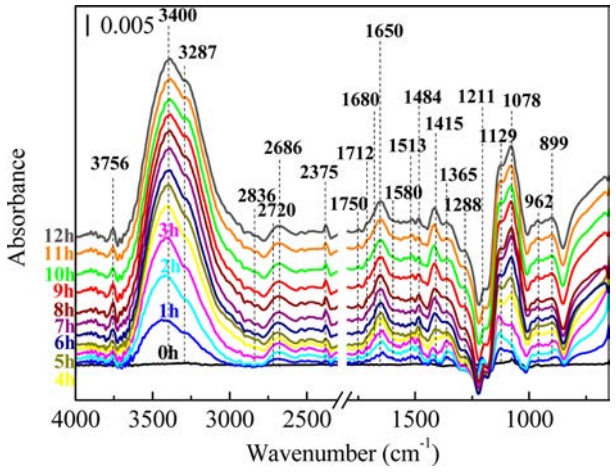

Figure 3. In situ FT-IR spectra during ozone oxidation of TMA exchanged $(NH_4)_2SO_4$. The initial O_3 concentration was 127 ppb.

means that TMA promotes the transformation of HSO_4^- to SO_4^{2-}, which is in agreement with our previous work in which no gas-phase NH_3 was detected by a mass spectrometer, and the transformation from HSO_4^- to SO_4^{2-} was observed using an in situ Raman spectrometer when NH_4HSO_4 was exposed to MA.[53]

It should be noted that protonated TMA ($(CH_3)_3NH^+$) was formed on all of these ammonium salts as both 1486 and 985 cm^{-1} bands were present in the corresponding IR spectra. This implies that aminium salts can be formed on all of these substrates. As shown in Figure 2, frequency shifts were observed for several IR bands of the exchanged TMA on different ammonium substrates. For example, the $2\delta_{as}$ (NC_3) band shifted from 845 cm^{-1}[48] on $(NH_4)_2SO_4$ and NH_4HSO_4 to 816 cm^{-1} on NH_4Cl and NH_4NO_3. The $\rho(CH_3)$ band was observed at 1259 cm^{-1} accompanied by new unknown bands at 1576 and 2608 cm^{-1} for TMA-exchanged NH_4Cl. This means that the structure of the formed $(HTMA)^+$ is sensitive to the surrounding anions.

Ozonolysis of Particulate TMA. To simplify the IR spectral analysis, the IR spectra were collected using the corresponding purged sample (TMA-exchanged ammonium salt) as a reference before O_3 was introduced into the reactor. Figure 3 shows the typical IR spectra during O_3 oxidation of TMA-exchanged $(NH_4)_2SO_4$. The O_3 concentration was 127 ppbv.

As shown in Figure 3, a number of new bands appeared and increased as a function of reaction time. The band at 3400 cm^{-1} with a shoulder at 3287 cm^{-1} and the peak 1649 cm^{-1} are the characteristic absorption bands of water.[49] Although the TMA exchanged particles were dried with zero air before O_3 oxidation, H_2O presenting in the gases (RH 12%) during ozonolysis of particulate TMA should lead to the increase in the IR intensity of water because the aminium salt was highly hygroscopic.[28] On the other hand, OH radical involved in the oxidation of amines.[34] Thus, H_2O formed through H-abstract reaction, which will be discussed later, might also contribute to the accumulation of water in the particle phase. The bands at 1750 (ν_s(C═O)), 1211 (δ(C−OH)) and 962 cm^{-1} (w_{oop}(CH), wag of CH out of plane) indicate the formation of formic acid.[54] Formaldehyde may also contribute to the absorbance band at 1750 cm^{-1} (ν_s(C═O)), which is accompanied by the $\nu_{as}(CH_2)$ band at 2836 cm^{-1} and ν_s(CH) at 2720 cm^{-1}[55] in Figure 3. The bands at 1660−1680 cm^{-1} can be assigned to the ν_s(C═O) of N,N-dimethylformamide (DMF), which is supported by the observation of ν_s(CN) at 1288 cm^{-1}, the r(CH_3) (rocking vibration of CH_3) at 1078 cm^{-1} and the mixing of $\delta(CH_3)$ and ν_s(CN) at 1513 cm^{-1} in DMF.[56] Monomethyleneamine ($CH_3N{=}CH_2$) was proposed as a possible product because the bands for β(C−H) (bending vibration in plane, 1415 cm^{-1}) of the $=CH_2$ group and ν_s(C−N) (899 cm^{-1}) were observable,[57] although it is hard to discern the ν_s(C═N) at around 1660 cm^{-1}[57] from bands of other species, including δ(OH) of water and ν_s(C═O) of formamide. As shown in Figure 3, nitromethane (CH_3NO_2) can be confirmed, with $\nu_{as}(NO_2)$ and $\nu_s(NO_2)$ at 1580 and 1365 cm^{-1},[58] respectively. The ν_s(CN) band of CH_3NO_2 at 885 cm^{-1}[58] was overlapped with ν_s(C−N) of $CH_3N{=}CH_2$ at 899 cm^{-1}.[57] The peaks at 1129 and 1484 cm^{-1} in Figure 3 should be related to the r(CH_3) and $\delta(CH_3)$ bands in nitromethane,[58] monomethyleneamine[57] and DMF.[56] The band at 2375 cm^{-1} is assigned to CO_2.[59] The peak at 3756 cm^{-1} implies that a compound containing OH was formed. In Figure 3, several negative peaks at 1230 cm^{-1} ($\rho(CH_3)$) and 845 cm^{-1} ($2\delta_{as}(NC_3)$)[48] were observed. This is consistent with the consumption of particle-phase TMA.

As discussed above, several possible products including H_2O, HCHO, HCOOH, $CH_3N{=}CH_2$, $HCON(CH_3)_2$ and CH_3NO_2 were detected, while some of their IR bands overlapped each other. Therefore, 2DCOS analyses were further performed to confirm the assignments for these species (Figure S3). Besides the bands observed in Figure 3, several new peaks, such as 3340, 3210, 2894, 2854, 2760, 2580, 1660, 1560, 1424, 1140, 921, 877, 820 cm^{-1}, have been identified in Figure S3 due to the higher spectral resolution of 2DCOS. As discussed in the SI, $(CH_3)_2NCHO$, CH_3NO_2, $CH_3N{=}CH_2$, HCHO and HCOOH were confirmed by 2DCOS although some peaks were overlapped. On the other hand, the IR frequencies of these products were consistent with DFT calculations and summarized in Table S2. The results further rationalized the assignment for the peaks identified in the IR spectra (Figures 3 and S3). In particular, the band at 3756 cm^{-1} was assigned to the ν_s(OH) of $CH_3N(OH)CHO$ or CH_3NHOH, which is close to the calculated value at 3677 cm^{-1} (3771 cm^{-1} with unscaled frequency) for $CH_3N(OH)$-CHO and 3730 cm^{-1} for CH_3NHOH, and the other IR bands

DOI: 10.1021/acs.est.6b04375
Environ. Sci. Technol. 2016, 50, 11076−11084

of $CH_3N(OH)CHO$ and CH_3NHOH were assigned and summarized in Table S2. This means that $CH_3N(OH)CHO$ or CH_3NHOH may be formed during ozonolysis of particulate TMA.

Figure 4 summarizes the IR spectra of the TMA-exchanged NH_4Cl, NH_4NO_3, and NH_4HSO_4 followed by O_3 oxidation for

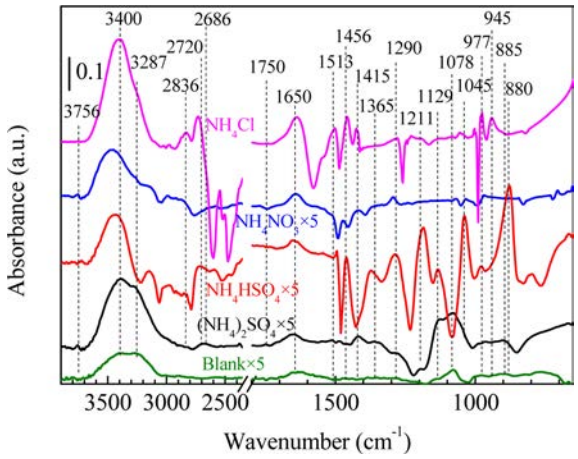

Figure 4. FT-IR spectra of TMA-exchanged NH_4Cl, NH_4NO_3, NH_4HSO_4 and $(NH_4)_2SO_4$ after being exposed to 267, 400, 203, 127 ppbv of ozone, respectively, for 12 h. The blank experiment was performed by exposing TMA absorbed on the cleaned ZnSe crystal (without ammonium) to 127 ppbv of ozone.

12 h. For comparison, the IR spectra of TMA-exchanged $(NH_4)_2SO_4$ and the blank experiment have also been included in the same figure. As shown in Figure 4, most of the species observed on TMA-exchanged $(NH_4)_2SO_4$ were present on the other ammonium salts, and the assignments of these species were summarized in Table S2 based on the literature and DFT calculations. Compared with ozone oxidation of the TMA-exchanged ammonium salts, oxidation of TMA absorbed on the blank ZnSe crystal (the cleaned ZnSe crystal without ammonium) showed little contribution to the IR signal. On the other hand, the IR signal during ozone oxidation of TMA-exchanged NH_4Cl or NH_4HSO_4 was much stronger than that of TMA-exchanged NH_4NO_3 or $(NH_4)_2SO_4$. This might result from different TMA contents obtained by the exchange reactions due to different reactivities between TMA and the ammonium salts as shown in Figure 2. The properties of anion ions may also have influence on the IR signals. For example, Cl^- does not have IR absorption in the range of 650−1800 cm^{-1}, which leading to a good spectral quality for NH_4Cl exchanged TMA. In addition, the difference in the IR signals among different substrates implies the different reactivity of particulate TMA toward O_3 due to the role of anion ions. It should be noted that an ATR accessory was used for IR spectra collection. The probe depth of the evanescent wave was less than 1.5 μm in the spectral region.[60] This means that particle-phase but not gas-phase products mainly contribute to the measured ATR-IR signals. In addition, oxidation of TMA exchanged $(NH_4)_2SO_4$ was further carried out in flow system, from which the species in the gas phase were flushed continuously. As show in Figure S4, the surface products were similar to that observed in the closed system. Therefore, it can be reasonably concluded that the observed products from ozonolysis of TMA were formed via heterogeneous oxidation of particle-phase TMA.

Figure 5 shows the mass spectra before and after O_3 oxidation of TMA-exchanged $(NH_4)_2SO_4$. After O_3 oxidation,

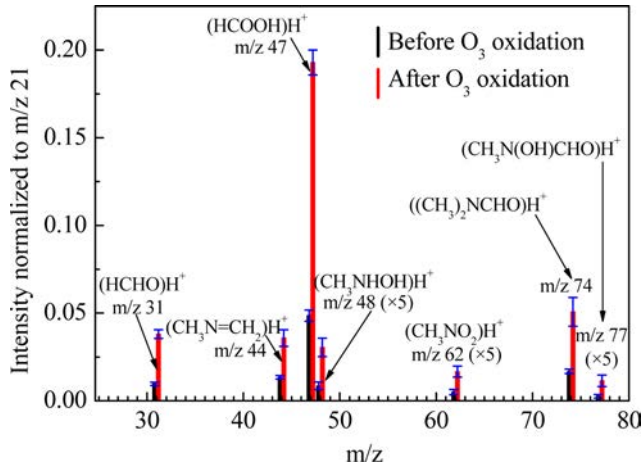

Figure 5. Intensity of selected mass channels before and after O_3 oxidation of TMA-exchanged $(NH_4)_2SO_4$ for 12 h with 127 ppbv of O_3.

the mass channels at m/z 31, 44, 47, 48, 62, 74, and 77 corresponding to $(HCHO)H^+$, $(CH_3N{=}CH_2)H^+$, $(HCOOH)H^+$, $(CH_3NHOH)H^+$, $(CH_3NO_2)H^+$, $((CH_3)_2NCHO)H^+$ and $(CH_3N(OH)CHO)H^+$, respectively, increased significantly. This was consistent with the result of in situ IR spectra and further confirmed HCHO, $CH_3N{=}CH_2$, HCOOH, CH_3NO_2, $(CH_3)_2NCHO$, CH_3NHOH and CH_3N-$(OH)CHO$ as oxidation products. These products are similar to those observed in the gas-phase oxidation of TMA by O_3.[34] One important observation is that most of these compounds (except for CH_3NHOH) could be still detected even when the oxidized sample had been purged with 1 L min^{-1} of zero air for 2 h (Figure S5). This indicated that a portion of these compounds were in the particle phase, and confirmed that these products were generated in the particle phase.

Oxidation Paths of Particulate TMA by Ozone. Based on the products observed in this work, the oxidation paths of particulate TMA by O_3 can be summarized in Figure 6. As shown in Figure S6, the symmetry of the highest occupied molecular orbital (HOMO) of TMA matches with that of the lowest unoccupied molecular orbital (LUMO) of O_3, while it does not between the HOMO of $TMAH^+$ and the LUMO of O_3. This means molecular TMA rather than $TMAH^+$ can be oxidized by O_3. Although it has been found that aminium sulfate is comparable or more thermostable than ammonium sulfate,[28] an equilibrium between molecular TMA and protonated TMA should be possible on the surface. Then, the N atom in TMA is attacked first by ozone followed by loss of oxygen, forming an energy-rich amine oxide similar to the mechanism described by Slagle et al.[61] for the reaction between O(3P) atoms and alkylamines. Nitromethane, which was identified as a product by both IR and PTR-MS in this study, is directly formed from the attack of amine oxide by a second ozone. Intramolecular H atom migration from the methyl group to the oxygen atom may occur and form an unstable hydroxylamine methyl radical. Thus, *N*-hydroxylmethylformamide is formed in the presence of O_2 by loss of a HO_2 radical from peroxide. $(CH_3)_2NCH_2$ radicals can be generated by H abstraction of TMA by OH radical or by loss of OH radical from the hydroxylamine. The corresponding peroxide radical

DOI: 10.1021/acs.est.6b04375
Environ. Sci. Technol. 2016, 50, 11076−11084

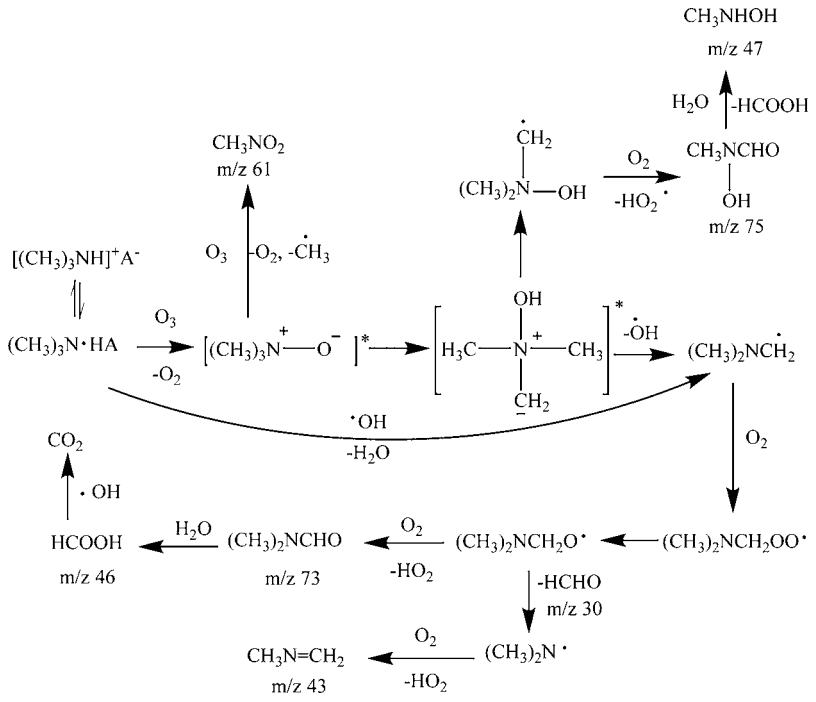

Figure 6. Possible oxidation paths of particulate TMA by ozone. "A" means anion.

$((CH_3)_2NCH_2O_2)$ and RO radical $((CH_3)_2NCH_2O)$ are formed in the presence of O_2. Finally, the $CH_3N{=}CH_2$ and $(CH_3)_2NCHO$ can be formed, accompanied by the loss of HCHO and/or HO_2 radical. HCOOH is produced from hydrolysis of $(CH_3)_2NCHO$ or CH_3NCHO and can be finally oxidized to CO_2. The oxidation mechanism of TMA in the particle phase (Figure 6) is similar to that in the gas phase.[34] However, besides oxidation reactions, hydrolysis in the particle phase has also been observed in this study. For example, a new product (CH_3NHOH) from hydrolysis of CH_3NCHO has been identified in the particle phase by both the IR and the PTR-MS.

■ ATMOSPHERIC IMPLICATIONS

As pointed out by Chapleski et al.[62] in a recent review paper, adsorption or uptake of volatile organic compounds onto liquid or solid surfaces is one of formation or growth mechanisms of organic particles in the atmosphere. Although the typical concentration of amines is from several pptv to tens of pptv,[63,64] it has been well recognized that amines contribute to both new particle formation[12,16] and brown carbon.[65] For example, nucleation rates with 5 pptv of DMA were enhanced more than 1000-fold compared with 250 pptv ammonia at ambient concentration of sulfuric acid.[16] On the other hand, although it has not been evaluated by modelers, heterogeneous uptake onto fine particles might also contribute to reduced nitrogen in particle phase due to the relative large uptake coefficients as reported previously.[22,53,66,67] Whatever the formation path is, once formed, organic nitrogen containing compounds including particulate amines nearly immediately begin the heterogeneous oxidation by oxidants in the lower atmosphere.[62]

The lifetimes of alkylamines exposed to ozone in the gas phase usually vary from a few hours to several days.[68] Although oxidized by OH is the dominant degradation path for amines, oxidation by O_3 may also be a degradation path for amines in the atmosphere. For example, the lifetimes of TEA, DEA, TMA, and DMA are in the range of 4.8−278 h under the typical tropospheric ozone concentration (7×10^{11} molecules cm^{-3}).[30] Products including HCHO, HCOOH, CH_3NO_2, $CH_3N{=}CH_2$, and $(CH_3)_2NCHO$ have been identified from ozonolysis of gas-phase amines.[34] As observed in this study, O_3 oxidation of particle-phase amines, which formed through heterogeneous uptake by ammonium, can also take place when exposed to O_3. HCHO, HCOOH, CH_3NO_2, $CH_3N{=}CH_2$ and $(CH_3)_2NCHO$ were confirmed as the major products by both FTIR and PTR-MS. Heterogeneous oxidation usually leads to increases in oxygen-containing species,[69,70] O/C ratio[71] and structure modifications of aerosol particles,[72] subsequently, may alter its hygroscopicity[73] and optical properties.[74] Although most of these products are volatile from ozone oxidation of particulate TMA, a portion of these compounds are in the particle phase. Thus, heterogeneous oxidation might have influence on the hygroscopic and optical properties of particulate amines, while further studies are required in the future. Because acid−base reactions between amines and inorganic or organic acids contribute to both the nucleation[12,16] and subsequent growth of submicron particles,[2] degradation of particle-phase amines might have a complex influence on air quality through changing their particulate lifetimes. It has been found that heterogeneous oxidation increased the redox activity[75−78] and the cytotoxicity[76,79,80] of black carbon. At the present time, it is poorly understood about the toxicological evolution during atmospheric aging of organic aerosol. However, HCHO, CH_3NO_2, and $(CH_3)_2NCHO$ from ozone oxidation of particulate TMA are well-recognized toxicants or carcinogens. Therefore, more attention should be paid to the health impacts of the secondary oxidation products from amines in the particle phase.

It should be pointed out that ozone concentration in this work were more representative of highly polluted locations and the particle size was 2−3 orders of magnitude greater than atmospheric particles. Because both the ozone concentration and the particle size should mainly have influence on the

DOI: 10.1021/acs.est.6b04375
Environ. Sci. Technol. 2016, 50, 11076−11084

reaction kinetics but not the reaction mechanism, the oxidation path observed in this work should have atmospheric relevance for understanding the fate of amines in the atmosphere. On the other hand, uptake coefficient of ozone on the particulate amines or degradation kinetics of particulate amines are very important to evaluate the atmospheric importance for the possible degradation paths proposed in this work. This requires further investigation of the degradation kinetics of particle-phase amines in the future.

■ ASSOCIATED CONTENT

Supporting Information

The Supporting Information is available free of charge on the ACS Publications website at DOI: 10.1021/acs.est.6b04375.

Interpretation of 2D correlation spectroscopy (2DCOS) data, reaction conditions in displacement and ozonolysis reactions, assignments of IR spectra, experimental setup, SEM micrographs of ammonium sulfate and aminium sulfate particles, 2DCOS, comparison between the in situ FT-IR spectra during ozone oxidation of TMA exchanged $(NH_4)_2SO_4$ in the flow system and the closed system and concentration changes of the products detected by the PTR-MS (PDF)

■ AUTHOR INFORMATION

Corresponding Author

*Phone: 86-10-62849337; fax: 86-10-62849121; e-mail: ycliu@rcees.ac.cn.

Notes

The authors declare no competing financial interest.

■ ACKNOWLEDGMENTS

This research was financially supported by the National Natural Science Foundation of China (41275131) and the Strategic Priority Research Program of Chinese Academy of Sciences (XDB05040100, XDB05010300).

■ REFERENCES

(1) Ge, X.; Wexler, A. S.; Clegg, S. L. Atmospheric amines - Part I. A review. *Atmos. Environ.* **2011**, *45* (3), 524−546.

(2) Qiu, C.; Zhang, R. Multiphase chemistry of atmospheric amines. *Phys. Chem. Chem. Phys.* **2013**, *15* (16), 5738−5752.

(3) Sellegri, K.; Hanke, M.; Umann, B.; Arnold, F.; Kulmala, M. Measurements of organic gases during aerosol formation events in the boreal forest atmosphere during QUEST. *Atmos. Chem. Phys.* **2005**, *5*, 373−384.

(4) Chang, S. G.; Novakov, T. Formation of pollution particulate nitrogen-compounds by no-soot and nh3-soot gas-particle surface-reactions. *Atmos. Environ.* **1975**, *9* (5), 495−504.

(5) Smith, J. N.; Dunn, M. J.; VanReken, T. M.; Iida, K.; Stolzenburg, M. R.; McMurry, P. H.; Huey, L. G., Chemical composition of atmospheric nanoparticles formed from nucleation in Tecamac, Mexico: Evidence for an important role for organic species in nanoparticle growth. *Geophys. Res. Lett.* **2008**, *35*, (4).10.1029/2007GL032523

(6) Novakov, T.; Mueller, P. K.; Alcocer, A. E.; Otvos, J. W. Chemical composition of Pasadena aerosol by particle size and time of day. III. Chemical states of nitrogen and sulfur by photoelectron spectroscopy. *J. Colloid Interface Sci.* **1972**, *39* (1), 225−234.

(7) Finessi, E.; Decesari, S.; Paglione, M.; Giulianelli, L.; Carbone, C.; Gilardoni, S.; Fuzzi, S.; Saarikoski, S.; Raatikainen, T.; Hillamo, R.; Allan, J.; Mentel, T. F.; Tiitta, P.; Laaksonen, A.; Petäjä, T.; Kulmala, M.; Worsnop, D. R.; Facchini, M. C. Determination of the biogenic secondary organic aerosol fraction in the boreal forest by NMR spectroscopy. *Atmos. Chem. Phys.* **2012**, *12* (2), 941−959.

(8) Laitinen, T.; Ehn, M.; Junninen, H.; Ruiz-Jimenez, J.; Parshintsev, J.; Hartonen, K.; Riekkola, M. L.; Worsnop, D. R.; Kulmala, M. Characterization of organic compounds in 10-to 50-nm aerosol particles in boreal forest with laser desorption-ionization aerosol mass spectrometer and comparison with other techniques. *Atmos. Environ.* **2011**, *45* (22), 3711−3719.

(9) Angelino, S.; Suess, D. T.; Prather, K. A. Formation of Aerosol Particles from Reactions of Secondary and Tertiary Alkylamines: Characterization by Aerosol Time-of-Flight Mass Spectrometry. *Environ. Sci. Technol.* **2001**, *35* (15), 3130−3138.

(10) Oezel, M. Z.; Ward, M. W.; Hamilton, J. F.; Lewis, A. C.; Raventos-Duran, T.; Harrison, R. M. Analysis of Organic Nitrogen Compounds in Urban Aerosol Samples Using GCxGC-TOF/MS. *Aerosol Sci. Technol.* **2010**, *44* (2), 109−116.

(11) Yu, H.; McGraw, R.; Lee, S.-H., Effects of amines on formation of sub-3 nm particles and their subsequent growth. *Geophys. Res. Lett.* **2012**, *39*.n/a10.1029/2011GL050099

(12) Smith, J. N.; Barsanti, K. C.; Friedli, H. R.; Ehn, M.; Kulmala, M.; Collins, D. R.; H.Scheckman, J.; Williams, B. J.; McMurry, P. H. Observations of aminium salts in atmospheric nanoparticles and possible climatic implications. *Proc. Natl. Acad. Sci. U. S. A.* **2010**, *107*, 6634−6639.

(13) Held, A.; Rathbone, G. J.; Smith, J. N. A Thermal desorption chemical ionization ion trap mass spectrometer for the chemical characterization of ultrafine aerosol particles. *Aerosol Sci. Technol.* **2009**, *43* (3), 264−272.

(14) Smith, J. N.; Moore, K. F.; McMurry, P. H.; Eisele, F. L. Atmospheric measurements of sub-20 nm diameter particle chemical composition by thermal desorption chemical ionization mass spectrometry. *Aerosol Sci. Technol.* **2004**, *38* (2), 100−110.

(15) Murphy, S. M.; Sorooshian, A.; Kroll, J. H.; Ng, N. L.; Chhabra, P.; Tong, C.; Surratt, J. D.; Knipping, E.; Flagan, R. C.; Seinfeld, J. H. Secondary aerosol formation from atmospheric reactions of aliphatic amines. *Atmos. Chem. Phys.* **2007**, *7* (9), 2313−2337.

(16) Almeida, J.; Schobesberger, S.; Kurten, A.; Ortega, I. K.; Kupiainen-Maatta, O.; Praplan, A. P.; Adamov, A.; Amorim, A.; Bianchi, F.; Breitenlechner, M.; David, A.; Dommen, J.; Donahue, N. M.; Downard, A.; Dunne, E.; Duplissy, J.; Ehrhart, S.; Flagan, R. C.; Franchin, A.; Guida, R.; Hakala, J.; Hansel, A.; Heinritzi, M.; Henschel, H.; Jokinen, T.; Junninen, H.; Kajos, M.; Kangasluoma, J.; Keskinen, H.; Kupc, A.; Kurten, T.; Kvashin, A. N.; Laaksonen, A.; Lehtipalo, K.; Leiminger, M.; Leppa, J.; Loukonen, V.; Makhmutov, V.; Mathot, S.; McGrath, M. J.; Nieminen, T.; Olenius, T.; Onnela, A.; Petaja, T.; Riccobono, F.; Riipinen, I.; Rissanen, M.; Rondo, L.; Ruuskanen, T.; Santos, F. D.; Sarnela, N.; Schallhart, S.; Schnitzhofer, R.; Seinfeld, J. H.; Simon, M.; Sipila, M.; Stozhkov, Y.; Stratmann, F.; Tome, A.; Trostl, J.; Tsagkogeorgas, G.; Vaattovaara, P.; Viisanen, Y.; Virtanen, A.; Vrtala, A.; Wagner, P. E.; Weingartner, E.; Wex, H.; Williamson, C.; Wimmer, D.; Ye, P.; Yli-Juuti, T.; Carslaw, K. S.; Kulmala, M.; Curtius, J.; Baltensperger, U.; Worsnop, D. R.; Vehkamaki, H.; Kirkby, J. Molecular understanding of sulphuric acid-amine particle nucleation in the atmosphere. *Nature* **2013**, *502* (7471), 359−363.

(17) Nishino, N.; Arquero, K. D.; Dawson, M. L.; Finlayson-Pitts, B. J. Infrared studies of the reaction of methanesulfonic acid with trimethylamine on surfaces. *Environ. Sci. Technol.* **2014**, *48*, 323−330.

(18) Chen, H.; Ezell, M. J.; Arquero, K. D.; Varner, M. E.; Dawson, M. L.; Gerber, R. B.; Finlayson-Pitts, B. J. New particle formation and growth from methanesulfonic acid, trimethylamine and water. *Phys. Chem. Chem. Phys.* **2015**, *17* (20), 13699−709.

(19) Nadykto, A. B.; Yu, F.; Jakovleva, M. V.; Herb, J.; Xu, Y. Amines in the Earth's atmosphere: A density functional theory study of the thermochemistry of pre-nucleation clusters. *Entropy* **2011**, *13*, 554−569.

(20) Kurtén, T.; Loukonen, V.; Vehkamöki, H.; Kulmala, M. Amines are likely to enhance neutral and ion-induced sulfuric acid-water nucleation in the atmosphere more effectively than ammonia. *Atmos. Chem. Phys.* **2008**, *8*, 4095−4103.

(21) Berndt, T.; Stratmann, F.; Sipilä, M.; Vanhanen, J.; Petäjä, T.; Mikkilä, J.; Grüner, A.; Spindler, G.; Lee Mauldin Iii, R.; Curtius, J.; Kulmala, M.; Heintzenberg, J. Laboratory study on new particle formation from the reaction OH + SO_2: influence of experimental conditions, H_2O vapour, NH_3 and the amine tert-butylamine on the overall process. *Atmos. Chem. Phys.* **2010**, *10* (15), 7101−7116.
(22) Bzdek, B. R.; Ridge, D. P.; Johnston, M. V. Amine exchange into ammonium bisulfate and ammonium nitrate nuclei. *Atmos. Chem. Phys.* **2010**, *10* (8), 3495−3503.
(23) Liu, Y.; Han, C.; Liu, C.; Ma, J.; Ma, Q.; He, H. Differences in the reactivity of ammonium salts with methylamine. *Atmos. Chem. Phys.* **2012**, *12* (11), 4855−4865.
(24) Chan, L. P.; Chan, C. K. Displacement of ammonium from aerosol particles by uptake of triethylamine. *Aerosol Sci. Technol.* **2012**, *46* (2), 236−247.
(25) Bzdek, B. R.; Ridge, D. P.; Johnston, M. V. Amine reactivity with charged sulfuric acid clusters. *Atmos. Chem. Phys.* **2011**, *11* (16), 8735−8743.
(26) Qiu, C.; Wang, L.; Lal, V.; Khalizov, A. F.; Zhang, R. Heterogeneous reactions of alkylamines with ammonium sulfate and ammonium bisulfate. *Environ. Sci. Technol.* **2011**, *45* (11), 4748−55.
(27) Liu, Y.; Ma, Q.; He, H. Heterogeneous uptake of amines by citric acid and humic acid. *Environ. Sci. Technol.* **2012**, *46* (20), 11112−8.
(28) Qiu, C.; Zhang, R. Physiochemical properties of alkylaminium sulfates: hygroscopicity, thermostability, and density. *Environ. Sci. Technol.* **2012**, *46* (8), 4474−4480.
(29) Atkinson, R. Kinetics and mechanisms of the gas-phase reactions of the hydroxyl radical with organic compounds under atmospheric conditions. *Chem. Rev.* **1986**, *85*, 69−201.
(30) Gai, Y.; Ge, M.; Wang, W. Rate constants for the gas phase reactions of ozone with diethylamine and triethylamine. *Chem. Phys. Lett.* **2010**, *26* (7), 1768−1772.
(31) Bailey, P. S.; Carter, T. P.; Southwick, L. M. Ozonation of amines. VI. Primary amines. *J. Org. Chem.* **1972**, *37* (19), 2997−3004.
(32) Bailey, P. S.; Lerdal, D. A.; Carter, T. P. Ozonation of nucleophiles 0.9. Tertiary-amines. *J. Org. Chem.* **1978**, *43* (13), 2662−2664.
(33) Bailey, P. S.; Southwick, L. M.; Carter, T. P. Ozonation of nucleophiles 0.8. Secondary-amines. *J. Org. Chem.* **1978**, *43* (13), 2657−2662.
(34) Tuazon, E. C.; Atkinson, R.; Aschmann, S. M.; Arey, J. Kinetics and products of the gas-phase reactions of O_3 with amines and related compounds. *Res. Chem. Intermed.* **1994**, *20* (3−5), 303−320.
(35) Hartwig, A.; et al. *The MAK Collection for Occupational Health and Safety*; Greim, H., Eds.; Wiley-VCH Verlag GmbH & Co. KGaA: Hoboken, NJ, 2005; pp 1−9.
(36) Guest, I.; Varma, D. R. Developmental toxicity of methylamines in mice. *J. Toxicol. Environ. Health* **1991**, *32* (3), 319−330.
(37) Guest, I.; Varma, D. R. Teratogenic and macromolecular-synthesis inhibitory effects of trimethylamine on mouse embryos in culture. *J. Toxicol. Environ. Health* **1992**, *36* (1), 27−41.
(38) Zahardis, J.; Geddes, S.; Petrucci, G. A. The ozonolysis of primary aliphatic amines in fine particles. *Atmos. Chem. Phys.* **2008**, *8* (5), 1181−1194.
(39) Fiala, E. S.; Czerniak, R.; Castonguay, A.; Conaway, C. C.; Rivenson, A. Assay of 1-nitropropane, 2-nitropropane, 1-azoxypropane and 2-azoxypropane for carcinogenicity by gavage in Sprague—Dawley rats. *Carcinogenesis* **1987**, *8* (12), 1947−1949.
(40) Blake, R. S.; Monks, P. S.; Ellis, A. M. Proton-transfer reaction mass spectrometry. *Chem. Rev.* **2009**, *109* (3), 861−896.
(41) Lindinger, W.; Hansel, A.; Jordan, A. On-line monitoring of volatile organic compounds at pptv levels by means of proton-transfer-reaction mass spectrometry (PTR-MS) - Medical applications, food control and environmental research. *Int. J. Mass Spectrom. Ion Processes* **1998**, *173* (3), 191−241.
(42) Hansel, A.; Jordan, A.; Holzinger, R.; Prazeller, P.; Vogel, W.; Lindinger, W. Proton-transfer reaction mass-spectrometry - online trace gas-analysis at the ppb level. *Int. J. Mass Spectrom. Ion Processes* **1995**, *149*, 609−619.
(43) Ozaki, Y.; Sasic, S.; Tanaka, T.; Noda, I. Two-dimensional correlation spectroscopy: Principle and recent theoretical development. *Bull. Chem. Soc. Jpn.* **2001**, *74* (1), 1−17.
(44) Noda, I. Two-dimensional infrared spectroscopy. *J. Am. Chem. Soc.* **1989**, *111* (21), 8116−8118.
(45) Harrington, P. d. B.; Urbas, A.; Tandler, P. J. Two-dimensional correlation analysis. *Chemom. Intell. Lab. Syst.* **2000**, *50* (2), 149−174.
(46) Noda, I. Two-dimensional correlation spectroscopy — Biannual survey 2007−2009. *J. Mol. Struct.* **2010**, *974*, 3−24.
(47) Cho, M. Coherent Two-Dimensional Optical Spectroscopy. *Chem. Rev.* **2008**, *108*, 1331−1418.
(48) Murphy, W. F.; Zerbetto, F.; Duncan, J. L.; McKean, D. C. Vibrational spectrum and harmonic force field of trimethylamine. *J. Phys. Chem.* **1993**, *97* (3), 581−595.
(49) Onasch, T. B.; Siefert, R. L.; Brooks, S. D.; Prenni, A. J.; Murray, B.; Wilson, M. A.; Tolbert, M. A. Infrared spectroscopic study of the deliquescence and efflorescence of ammonium sulfate aerosol as a function of temperature. *J. Geophys. Res.-Atmos.* **1999**, *104* (D17), 21317−21326.
(50) Miller, F. A.; Wilkins, C. H. Infrared spectra and characteristic frequencies of inorganic ions. *Anal. Chem.* **1952**, *24* (8), 1253−1294.
(51) Lloyd, J. A.; Heaton, K. J.; Johnston, M. V. Reactive uptake of trimethylamine into ammonium nitrate particles. *J. Phys. Chem. A* **2009**, *113* (17), 4840−4843.
(52) Ongwandee, M.; Morrison, G. C.; Guo, X.; Chusuei, C. C. Adsorption of trimethylamine on zirconium silicate and polyethylene powder surfaces. *Colloids Surf., A* **2007**, *310* (1−3), 62−67.
(53) Liu, Y.; Han, C.; Liu, C.; Ma, J.; Ma, Q.; He, H. Differences in the reactivity of ammonium salts with methylamine. *Atmos. Chem. Phys.* **2012**, *12* (11), 4855−4865.
(54) Pettersson, M.; Lundell, J.; Khriachtchev, L.; Räsänen, M. IR spectrum of the other rotamer of formic acid, *cis*-HCOOH. *J. Am. Chem. Soc.* **1997**, *119* (48), 11715−11716.
(55) Busca, G.; Lamotte, J.; Lavalley, J. C.; Lorenzelli, V. FT-IR study of the adsorption and transformation of formaldehyde on oxide surfaces. *J. Am. Chem. Soc.* **1987**, *109* (17), 5197−5202.
(56) Durgaprasad, G.; Sathyanarayana, D. N.; Patel, C. C. Infrared spectra and normal vibrations of n,n-dimethylformamide and N,N-dimethylthioformamide. *Bull. Chem. Soc. Jpn.* **1971**, *44* (2), 316−322.
(57) Lindley, C., The kinetics of dimethylamino radical reactions in simulated atmospheres: The formation of dimethylnitrosamine and dimethylnitramine. Ph.D. Dissertation. Ohio State University, Columbus, OH, 1978.
(58) Itoh, K.; Iwa, A.; Uriu, Y.; Kadokura, K. Infrared absorption spectroscopic and DFT calculation studies on the adsorption structures of nitromethane on the single crystals of Cu and Ag. *Surf. Sci.* **2008**, *602* (13), 2148−2156.
(59) Liu, Y.; He, H.; Xu, W.; Yu, Y. Mechanism of Heterogeneous reaction of carbonyl sulfide on magnesium oxide. *J. Phys. Chem. A* **2007**, *111*, 4333−4339.
(60) Öhman, M.; Persson, D.; Leygraf, C. In situ ATR-FTIR studies of the aluminium/polymer interface upon exposure to water and electrolyte. *Prog. Org. Coat.* **2006**, *57* (1), 78−88.
(61) Atkinson, R.; Pitts, J. N. Kinetics of the reactions of O(^{3}P) atoms with the amines CH_3NH_2, $C_2H_5NH_2$, $(CH_3)_2NH$, and $(CH_3)_3N$ over the temperature range 298−440 K. *J. Chem. Phys.* **1978**, *68* (3), 911.
(62) Jr, R. C. C.; Zhang, Y.; Troya, D.; Morris, J. R. Heterogeneous chemistry and reaction dynamics of the atmospheric oxidants, O_3, NO_3, and OH on organic surfaces. *Chem. Soc. Rev.* **2016**, *45*, 3731−3746.
(63) You, Y.; Kanawade, V. P.; de Gouw, J. A.; Guenther, A. B.; Madronich, S.; Sierra-Hernández, M. R.; Lawler, M.; Smith, J. N.; Takahama, S.; Ruggeri, G.; Koss, A.; Olson, K.; Baumann, K.; Weber, R. J.; Nenes, A.; Guo, H.; Edgerton, E. S.; Porcelli, L.; Brune, W. H.; Goldstein, A. H.; Lee, S. H. Atmospheric amines and ammonia

DOI: 10.1021/acs.est.6b04375
Environ. Sci. Technol. 2016, 50, 11076−11084

measured with a chemical ionization mass spectrometer (CIMS). *Atmos. Chem. Phys.* **2014**, *14* (22), 12181−12194.
(64) Hellén, H.; Kieloaho, A. J.; Hakola, H. Gas-phase alkyl amines in urban air; comparison with a boreal forest site and importance for local atmospheric chemistry. *Atmos. Environ.* **2014**, *94* (0), 192−197.
(65) Zarzana, K. J.; De Haan, D. O.; Freedman, M. A.; Hasenkopf, C. A.; Tolbert, M. A. Optical Properties of the Products of α-Dicarbonyl and Amine Reactions in Simulated Cloud Droplets. *Environ. Sci. Technol.* **2012**, *46* (9), 4845−4851.
(66) Qiu, C.; Wang, L.; Lal, V.; Khalizov, A. F.; Zhang, R. Heterogeneous reactions of alkylamines with ammonium sulfate and ammonium bisulfate. *Environ. Sci. Technol.* **2011**, *45*, 4748−4755.
(67) Liu, Y.; Ma, Q.; He, H. Heterogeneous uptake of amines by citric acid and humid acid. *Environ. Sci. Technol.* **2012**, *46*, 11112−11118.
(68) Nielsen, C. J.; Herrmann, H.; Weller, C. Atmospheric chemistry and environmental impact of the use of amines in carbon capture and storage (CCS). *Chem. Soc. Rev.* **2012**, *41* (19), 6684−6704.
(69) Chughtai, A. R.; Jassim, J. A.; Peterson, J. H.; Stedman, D. H.; Smith, D. M. Spectroscopic and Solubility Characteristics of Oxidized Soots. *Aerosol Sci. Technol.* **1991**, *15*, 112−126.
(70) Mawhinney, D. B.; Naumenko, V.; Kuznetsova, A.; Yates, J. T.; Liu, J.; Smalley, R. E. Infrared spectral evidence for the etching of carbon nanotubes: Ozone oxidation at 298 K. *J. Am. Chem. Soc.* **2000**, *122* (10), 2383−2384.
(71) Jimenez, J. L.; Canagaratna, M. R.; Donahue, N. M.; Prevot, A. S. H.; Zhang, Q.; Kroll, J. H.; DeCarlo, P. F.; Allan, J. D.; Coe, H.; Ng, N. L.; Aiken, A. C.; Docherty, K. S.; Ulbrich, I. M.; Grieshop, A. P.; Robinson, A. L.; Duplissy, J.; Smith, J. D.; Wilson, K. R.; Lanz, V. A.; Hueglin, C.; Sun, Y. L.; Tian, J.; Laaksonen, A.; Raatikainen, T.; Rautiainen, J.; Vaattovaara, P.; Ehn, M.; Kulmala, M.; Tomlinson, J. M.; Collins, D. R.; Cubison, M. J.; Dunlea, E. J.; Huffman, J. A.; Onasch, T. B.; Alfarra, M. R.; Williams, P. I.; Bower, K.; Kondo, Y.; Schneider, J.; Drewnick, F.; Borrmann, S.; Weimer, S.; Demerjian, K.; Salcedo, D.; Cottrell, L.; Griffin, R.; Takami, A.; Miyoshi, T.; Hatakeyama, S.; Shimono, A.; Sun, J. Y.; Zhang, Y. M.; Dzepina, K.; Kimmel, J. R.; Sueper, D.; Jayne, J. T.; Herndon, S. C.; Trimborn, A. M.; Williams, L. R.; Wood, E. C.; Middlebrook, A. M.; Kolb, C. E.; Baltensperger, U.; Worsnop, D. R. Evolution of Organic Aerosols in the Atmosphere. *Science* **2009**, *326*, 1525−1529.
(72) Qiu, C.; Khalizov, A. F.; Zhang, R. Soot Aging from OH-Initiated Oxidation of Toluene. *Environ. Sci. Technol.* **2012**, *46* (17), 9464−9472.
(73) Petters, M. D.; Prenni, A. J.; Kreidenweis, S. M.; DeMott, P. J.; Matsunaga, A.; Lim, Y. B.; Ziemann, P. J. Chemical aging and the hydrophobic-to-hydrophilic conversion of carbonaceous aerosol. *Geophys. Res. Lett.* **2006**, *33* (24), L24806.
(74) Lambe, A. T.; Cappa, C. D.; Massoli, P.; Onasch, T. B.; Forestieri, S. D.; Martin, A. T.; Cummings, M. J.; Croasdale, D. R.; Brune, W. H.; Worsnop, D. R.; Davidovits, P. Relationship between oxidation level and optical properties of secondary organic aerosol. *Environ. Sci. Technol.* **2013**, *47* (12), 6349−6357.
(75) Li, Q.; Shang, J.; Zhu, T. Physicochemical characteristics and toxic effects of ozone-oxidized black carbon particles. *Atmos. Environ.* **2013**, *81* (0), 68−75.
(76) Holder, A. L.; Carter, B. J.; Goth−Goldstein, R.; Lucas, D.; Koshland, C. P. Increased cytotoxicity of oxidized flame soot. *Atmos. Pollut. Res.* **2012**, *3*, 25−31.
(77) McWhinney, R. D.; Badali, K.; Liggio, J.; Li, S.-M.; Abbatt, J. P. D. Filterable redox cycling activity: a comparison between diesel exhaust particles and secondary organic aerosol constituents. *Environ. Sci. Technol.* **2013**, *47* (7), 3362−3369.
(78) McWhinney, R. D.; Gao, S. S.; Zhou, S.; Abbatt, J. P. D. Evaluation of the effects of ozone oxidation on redox-cycling activity of two-stroke engine exhaust particles. *Environ. Sci. Technol.* **2011**, *45*, 2131−2136.
(79) Kumarathasan, P.; Das, D.; Salam, M. A.; Mohottalage, S.; DeSilva, N.; Simard, B.; Vincent, R. Mass spectrometry-based proteomic assessment of the in vitro toxicity of carbon nanotubes. *Current Topics Biochem. Res.* **2012**, *14* (1), 15−27.
(80) Bottini, M.; Bruckner, S.; Nika, K.; Bottini, N.; Bellucci, S.; Magrini, A.; Bergamaschi, A.; Mustelin, T. Multi-walled carbon nanotubes induce T lymphocyte apoptosis. *Toxicol. Lett.* **2006**, *160* (2), 121−126.

DOI: 10.1021/acs.est.6b04375
Environ. Sci. Technol. 2016, 50, 11076−11084